LA-4008

LOS ALAMOS SCIENTIFIC LABORATORY
of the
University of California
LOS ALAMOS • NEW MEXICO

Measurement of Carbon Gradient in Stainless Steel by ^{3}He Activation and Autoradiography

UNITED STATES
ATOMIC ENERGY COMMISSION
CONTRACT W-7405-ENG. 36

DISCLAIMER

Printed in the United States of America. Available from
Clearinghouse for Federal Scientific and Technical Information
National Bureau of Standards, U. S. Department of Commerce
Springfield, Virginia 22151
Price: Printed Copy $3.00; Microfiche $0.65

LA-4008
UC-25, METALS, CERAMICS,
AND MATERIALS
TID-4500

LOS ALAMOS SCIENTIFIC LABORATORY
of the
University of California
LOS ALAMOS • NEW MEXICO

Report written: April 1968
Report distributed: December 20, 1968

Measurement of Carbon Gradient in Stainless Steel by ^3He Activation and Autoradiography

by

Jack L. Parker

Dale M. Holm

THIS PAGE

WAS INTENTIONALLY

LEFT BLANK

MEASUREMENT OF CARBON GRADIENT IN STAINLESS STEEL BY ^{3}He ACTIVATION AND AUTORADIOGRAPHY

by

Jack L. Parker and Dale M. Holm

ABSTRACT

A method combining activation by ^{3}He irradiation with autoradiographic techniques has been demonstrated to give good measurements of both carbon concentration and carbon gradients in stainless steel. Carbon in the surface of the sample is first activated by the $^{12}C(^{3}He,^{4}He)^{11}C$ reaction (^{3}He energy of ≈6.5 MeV). Autoradiographs of the activated surface are then made, the exposure being mainly by the positrons from the decay of the ^{11}C (^{11}C 20.4 min $^{11}B + \beta^{+} + \nu$). Densitometric analysis of the autoradiographs together with a measurement of the ^{11}C activity induced in the sample and a knowledge of reaction cross section, particle range, and other parameters are used in the computations. The technique is applicable to the determination of carbon distributions in matrices with $Z \geq 25$.

INTRODUCTION

Activation analysis with ^{3}He ions has been demonstrated by Markowitz and Mahony[1,2] to be a very sensitive method for measuring the concentrations of elements of low atomic number in matrices of high atomic number. Carbon is among the elements easily and conveniently detected by this method. The short range of the ^{3}He ions in solid samples and the strong energy dependence of the cross sections confine the activation to a thin surface layer (which is typical of the bulk of the sample if surface contamination is negligible). By combining the techniques of autoradiography with activation analysis, a map of the carbon concentration in the surface of a sample of steel (or any other appropriate matrix) can be obtained.

^{3}He activation is currently under investigation at the Los Alamos Scientific Laboratory as a means of determining carbon concentrations and gradients in stainless steel cladding for carbide reactor fuels.

Basically, the method[3,4] consists of first activating a fraction of the carbon in the surface of the sample by the $^{12}C(^{3}He,^{4}He)^{11}C$ reaction. Then one or more autoradiographs are made by exposing nuclear track plates to the irradiated sample. Positrons from the decay of ^{11}C (20.4-min half-life) pass through the photographic emulsion and deposit a small amount of energy in transit. This energy deposition makes the emulsion grains developable. The decay curve of the activated sample is obtained concurrently with the photographic exposure by counting the coincidence pairs of 0.51-MeV gamma rays from positron annihilation.

The decay curve, together with knowledge of beam current, reaction cross section, irradiation time, and the range of ^{3}He in the sample, gives the average concentration of carbon in the irradiated area. The autoradiographs, when interpreted by means of photographic density measurements and an emulsion calibration, give the relative carbon concentration as a function of position. Combining the results from the decay curve and autoradiographs gives absolute concentration as a function of position. Absolute concentrations can also be determined by comparing autoradiographs from samples of known carbon content with those from samples with unknown carbon distributions.

THEORETICAL

Since the electronic repulsion (Coulomb barrier) of a nucleus increases with increasing atomic number (hereafter designated by the usual notation, Z), charged particle activation analysis can be used to detect elements of low Z in matrices of higher Z.[5] The energy of the activating particle must be chosen so that it is greater than the Coulomb barrier of the low-Z element under analysis but less than the barrier energy of the higher Z matrix element (or elements). Because of the barrier, the bombarding particles rarely come close enough to the matrix nuclei to interact with them, and the low-Z nuclei are preferentially activated to a degree depending on the difference in Z. The quantum mechanical tunneling effect (whereby a particle with less than barrier energy has, nevertheless, a small probability of penetrating the barrier) and the concentration of the element to be analyzed determine the minimum difference in Z for which activation analysis may be carried out without undue interference from matrix activation.

The magnitude of the Coulomb barrier is given by

$$V_B = \frac{Z_1 Z_2 e^2}{R}, \qquad (1)$$

where Z_1 and Z_2 are the atomic numbers of the projectile and target, respectively, and e is the charge on the electron. R is the effective nuclear radius (the separation distance to which projectile must penetrate in order to interact), given by

$$R = 1.5 \times 10^{-13}\left(A_1^{1/3} + A_2^{2/3}\right), \qquad (2)$$

where A_1 and A_2 are the respective atomic weights of projectile and target nuclei. In general, $A_1 << A_2$ and $Z_2 \approx A_2/2$, and therefore the barrier energy is roughly proportional to $Z_2^{2/3}$.

Many of the reactions of ^{3}He with low-Z elements produce energy (i.e., are exothermic reactions). For example, in the $^{12}C(^3He, ^4He)^{11}C$ reaction, 1.85 MeV of energy is produced. Therefore, if the bombarding ion can penetrate the nucleus by tunneling or surmounting the barrier, there is a high probability that the reaction will take place. Figure 1 shows that tunneling is not very important because the cross section becomes significant just above the Coulomb barrier energy of 3.1 MeV. The cross section rises rapidly for several MeV to a maximum value. The decline from the maximum is also typical and is caused by increasing competition with other reactions which become more probable at higher ^{3}He energies.

These considerations give some insight into the factors involved in ^{3}He activation analysis. They imply that, in the detection of carbon, concentrations as low as ≈10 ppm can be measured in matrices of $Z \geq 25$ with little interference from matrix activation if the ^{3}He energy is ≈6 MeV. A Van de Graaff accelerator capable of 3 MV can give 6-MeV energy to doubly ionized $^3He^{2+}$ particles.

The fundamental relation used in determining the average concentration of carbon in the irradiated area is

$$\bar{N} = \frac{A}{\eta\, \bar{\sigma}\, R(1 - e^{-\lambda t})}, \qquad (3)$$

where

$\bar{N}$ = average number of carbon nuclei per cm^3

A = decay rate of carbon at end of irradiation

η = number of ^{3}He nuclei striking sample each second (must be kept constant throughout the irradiation if the relationship is to hold)

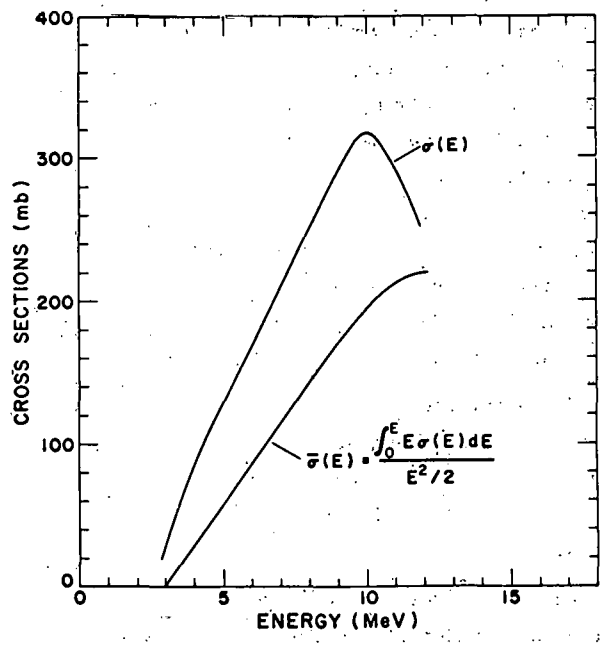

Fig. 1. Cross sections and average cross section for the $^{12}C(^3He, ^4He)^{11}C$ reaction.

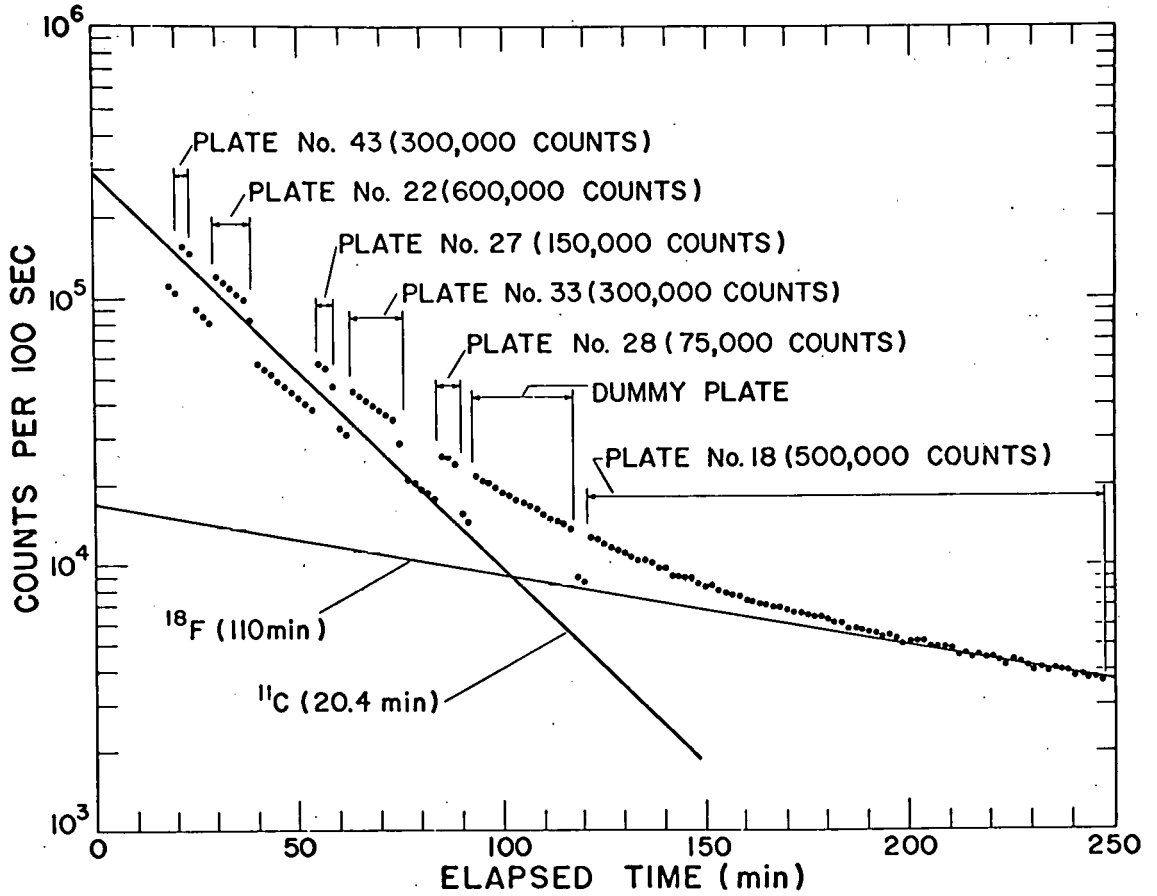

Fig. 2. Decay curve for stainless steel specimen after irradiation.

$\bar{\sigma}$ = average cross section for the reaction (function of ^{3}He energy)

R = ^{3}He range in sample for the energy used

$\lambda = 0.693/T_{\frac{1}{2}}$ = decay constant for ^{11}C

t = duration of irradiation

Several of the quantities in Eq. 3 need further comment. The activity, A, at the end of the irradiation, is found by fitting the decay curve and extrapolating to the end of irradiation. Figure 2 is an example of a two-component curve.

In order to get the true activity, the efficiency of the coincidence counting system must be known. For simple one- or even two-component curves, the fitting may be done by eye with reasonable accuracy. Where accuracy is important and for more complex curves, computer analysis, usually by the method of least squares, becomes essential.

The average cross section is given to a good approximation by[6]

$$\bar{\sigma}(\varepsilon) = (2/\varepsilon^2) \int_0^{\varepsilon} \sigma(E)\, E\, dE \,, \qquad (4)$$

where $\sigma(E)$ is the differential cross section for the reaction and ε is the energy of irradiation. For the $^{12}C(^3He,^4He)^{11}C$ reaction, $\sigma(E)$ and $\bar{\sigma}(\varepsilon)$ are shown in Fig. 1. Because of difficulties in measurement, the uncertainty in $\bar{\sigma}(\varepsilon)$ is probably at least $\pm$10%. The range, R, as a function of energy may be found in various compilations.[7,8] Because of experimental and computational difficulties, R may also be uncertain by $\pm$10%. When all the uncertainties are considered, N determined by Eq. 3 is probably uncertain by ≈20%.

EXPERIMENTAL

A test sample was prepared by encapsulating uranium carbide pellets and 2 g of sodium in a 1/2-in.-diam, 0.063-in.-wall, Type 316 stainless steel

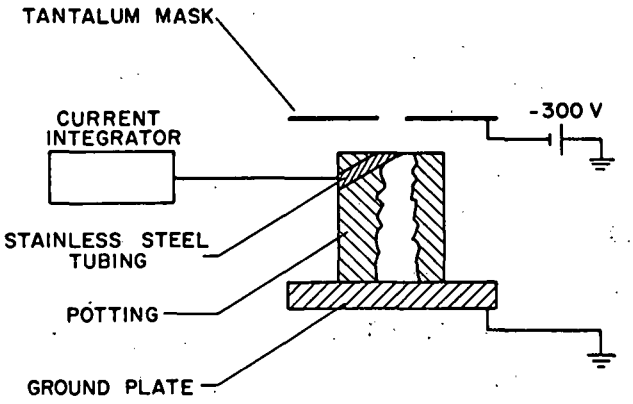

Fig. 3. Schematic of irradiation geometry.

capsule. This capsule was heated in an inert atmosphere for 96 h at 750°C. After test, analysis of the sodium showed that it contained 150 ppm carbon. The tubing was cut at an angle of ≈30° with respect to its own axis, potted, and polished. It was then mounted for irradiation, as shown in Fig. 3. A tantalum mask defined the 1.25 x 2.50 mm area to be irradiated. Larger areas can be irradiated uniformly by using two-dimensional beam sweeping techniques, but the average beam density is decreased.

The sample was irradiated for 40 min in a Van de Graaff generator with 20 nA of 6.5-MeV $^{3}He^{2+}$ ions (machine energy 3.25 MV). As previously explained, the energy of 6.5 MeV was a compromise dictated by the desire to have as high a cross section as possible for ^{11}C production and by the necessity of avoiding significant activation of the iron in the steel. Inasmuch as the sample was known to have a maximum carbon concentration of about 1%, 20 nA was adequate $^{3}He^{2+}$ beam current to give sufficient activation.

The decay curve (Fig. 2) was obtained by counting in coincidence the 0.51-MeV gamma pairs from the annihilation of the positrons. The counting systems consisted of two 3-in.-diam by 3-in.-long NaI crystals about 1.5 in. apart. When the irradiated area was covered by a Kodak NTB plate (0.065-in.-thick glass with 10-μ emulsion), all the gamma pairs came from what was nearly a point source because of the short range of the positrons in glass. The efficiency for this arrangement was ≈5%. A counting interval of 100 sec was used (≈12 intervals per half-life of ^{11}C).

Six autoradiographs of the stainless steel tubing were made during the intervals indicated in Fig. 2. The "steps" in the curve are caused by the escape of some positrons from between the NaI crystals during intervals when no autoradiographic plate was on the sample. The positrons have a range of several centimeters in air and generally do not annihilate until they come to rest. The 110-min component of the curve is from the decay of ^{18}F from the reaction $^{16}O(^{3}He,p)^{18}F$. It is present mainly because the irradiated area contained a crack filled with oxygen- and carbon-bearing potting or grinding compound. Stainless steels also contain randomly distributed crystals of chromates or silicates which will cause black spots in autoradiographs and give a small 110-min component to the decay curve. Such spots from oxygen activation are seen in the autoradiograph of plate 18 in Fig. 4. (The exposure of the plates was measured by counting for a predetermined number of gamma coincidences.)

Although the annihilation of each positron produces a pair of 0.51-MeV gamma rays, the emulsion used is much more sensitive to electrons or positrons than to gamma rays. Thus, the autoradiograph is not blurred significantly by the annihilation radiation.

The resolution of detail obtainable in the autoradiographs is a function of ^{3}He range in the sample, the positron range in both the sample and the autoradiographic plates, and emulsion thickness. The range of a 6-MeV ^{3}He ion in iron is about 0.001 in., and the range of the maximum energy positron is at least several times that. (The maximum energy of the positrons from ^{11}C is 0.96 MeV, and that from ^{15}O is 1.74 MeV.) In general, the positrons expend only a small amount of energy in traversing the nuclear emulsion, and it takes about 10 positrons passing through a grain to render the grain developable.

Figure 4 shows two autoradiographs and a photomicrograph of the irradiated area of the sample. Note that the irradiated area has been rendered visible by the ion bombardment. Also note the crack at the lower right of the irradiated area.

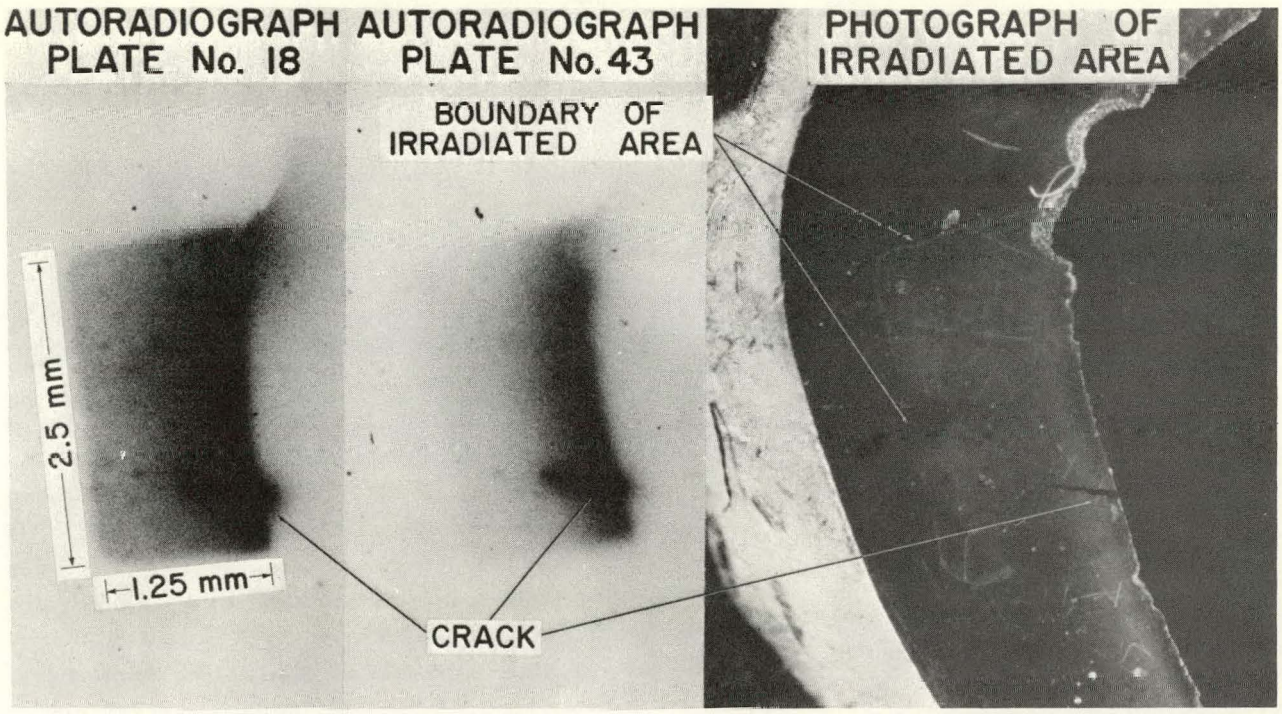

Fig. 4. Autoradiograph and photomicrograph of irradiated portion of stainless steel specimen.

The intense exposure due to the activated oxygen and carbon in the crack is evident in the autoradiographs. Qualitatively, the carbon gradient in the stainless steel is evident in both autoradiographs.

For quantitative determinations of the carbon gradient, densitometer traverses were made at about the center of each autoradiograph in the direction of the gradient. Figure 5 is a typical densitometer trace. (The densitometer aperture was 0.0005 by 0.015 cm.) The lack of sharpness in the density cutoff at both sides of the irradiated area is due to the particle ranges discussed above. In addition, at the high-density side of the densitometer trace, some positrons found long paths through air from the unpotted edge of the irradiated sample to the emulsion, thus making a more gradual cutoff.

In obtaining the relative concentration of carbon, one must know the relationship between photographic density (roughly the degree of blackening of the plate) and the exposure. This relationship is nonlinear and must be established experimentally. Figure 6 is an example of this relationship for Kodak NTB emulsion exposed to a ^{182}Ta β^- source. Because small differences in processing produce differences in the calibration curve, calibration plates and autoradiograph plates should be from the same emulsion batch and should be processed together. In this experiment, the calibration plate for comparison with the NTB plates was made <u>after</u> the actual autoradiographs were exposed and developed. This was unfortunate but necessary, because appropriate exposures had to be determined by trial and

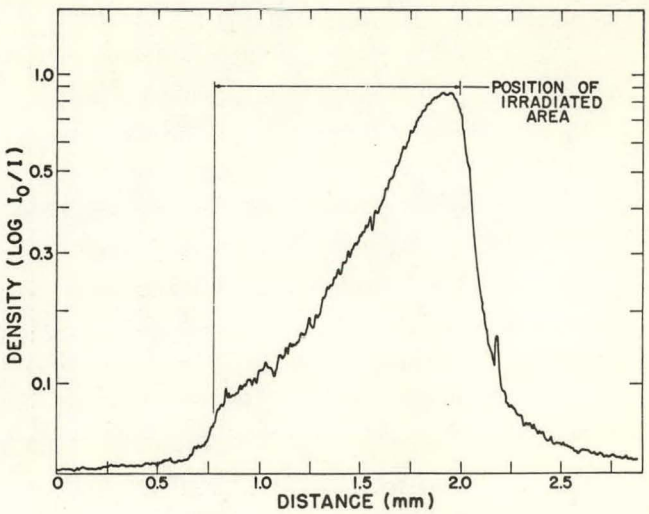

Fig. 5. Densitometer trace of autoradiograph taken from activated stainless steel specimen.

error. Thus, the calibration curve (Fig. 6) applies to the various autoradiographs with varying degrees of accuracy because of minor differences in exposure and development among them.

This approximate calibration curve, when applied to three of the autoradiographs, gives the results shown in Fig. 7. Considering the variations in exposure and development of the autoradiographs, the results are quite consistent for the sample of Fig. 4. It is obvious that, for the relative exposures to be directly proportional to the carbon concentration, the irradiation must be uniform over the irradiated area. Accurate determination of the average carbon concentration from the decay curve was not possible because of the unknown contribution to the decay curve from the irradiated material in the crack. However, it can be concluded from the data that the average carbon concentration is ≈1.7% and the maximum at the inner surface of the sample is ≈5%. These values are consistent with the carburization conditions.

The relative concentrations determined by densitometry of the autoradiographs can be made quantitative in at least two ways. If samples of the matrix material with a known, uniform carbon distribution are available, they can be irradiated identically to the unknown samples, and calibration exposures can be made from them. If such samples are not available or can not be irradiated conveniently, the average concentration over the area can be determined by the method used in the example above.

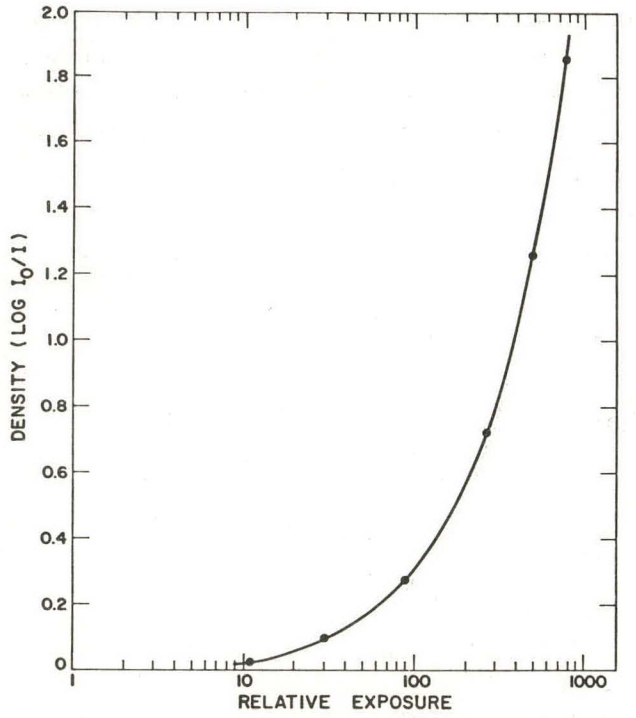

Fig. 6. Typical calibration curve for Kodak NTB nuclear track plates.

CONCLUSIONS

This exploratory experiment shows clearly that precise measurements of carbon concentration and gradients in stainless steel can be obtained by the technique described. The carbon gradient measured ranged from about 500 to 5000 ppm, but concentrations as low as 100 ppm should be easily measurable under the conditions of these experiments. By increasing irradiation time and beam current and by using a more sensitive emulsion,[9,10] the sensitivity could be increased by about a factor of ten. The limiting factor is in obtaining sufficient β^+ activity to expose the autoradiograph. Enough activity for reasonable decay curves can be obtained at a much lower carbon level. The method can be extended to obtaining gradients for two impurities, if their half-lives are sufficiently different, by comparing autoradiographs made at different times.

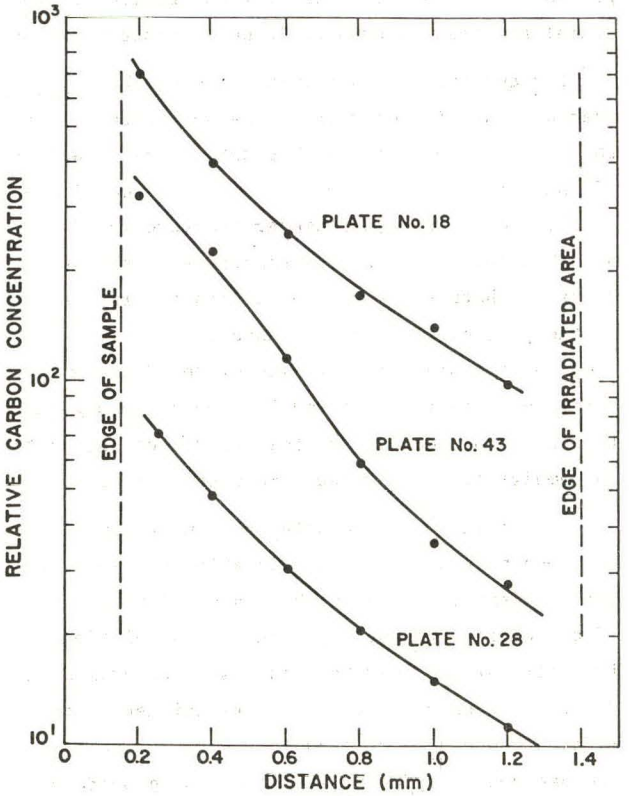

Fig. 7. Relative carbon gradient in sample as determined from three autoradiographs.

ACKNOWLEDGMENT

The sample of stainless steel tubing was carburized by Felix Litton of this Laboratory.

REFERENCES

1. S. S. Markowitz and J. D. Mahony, Anal. Chem. 34, 329 (1962).

2. S. S. Markowitz and J. D. Mahony, "^{3}He Activation Analysis for Carbon by $^{12}C(^{3}He,^{4}He)^{11}C$ Reaction," Radiochemical Methods of Analysis, Proc. Symp. Salzburg, Austria, 1964, Vol. 1, 1965, p. 419.

3. Dale M. Holm, J. A. Basmajian, and Wm. Mort Sanders, "Observation of the Microscopic Distribution of Oxygen and Carbon in Metals by ^{3}He Activation," LA-3515, Los Alamos Scientific Laboratory (1966).

4. D. M. Holm, W. L. Briscoe, J. L. Parker, and W. M. Sanders, IEEE Trans. Nucl. Sci. 15, 438 (1968).

5. R. S. Tilbury, "Activation Analysis with Charged Particles," NAS-NS 3110, National Academy of Sciences (1966).

6. E. Ricci and R. L. Hahn, Anal. Chem. 37, 743 (1965).

7. Andre C. Demildt, "Range-Energy Relations of ^{3}He Calculated for Several Elements," UCRL-10647, University of California Radiation Laboratory, Berkeley (1963).

8. C. Williamson and J. P. Boujot, "Tables of Range and Rate of Energy Loss of Charged Particles of Energy 0.5 to 150 MeV," CEA-2189, Centre d'Etudes Nucleaires de Saclay, France (1962).

9. Walter S. Barkas, Nuclear Research Emulsions, Academic Press, New York, 1963, Chapter 1.

10. "Kodak Materials for Nuclear Physics and Autoradiography," Kodak Pamphlet P-64 (1965).